

An OSp extension of the canonical tensor model

Gaurav Narain^{1,*} and Naoki Sasakura^{2,*}

¹Max-Planck-Institut für Gravitationsphysik (Albert-Einstein-Institut), Am Mühlenberg 1, D-14476 Potsdam-Golm, Germany

²Yukawa Institute for Theoretical Physics, Kyoto University, Oiwake-cho, Kitashirakawa, Sakyo-ku, Kyoto, 606-8502, Japan

*E-mail: gaunarain@gmail.com, sasakura@yukawa.kyoto-u.ac.jp

Received September 25, 2015; Accepted October 26, 2015; Published December 21, 2015

.....

Tensor models are generalizations of matrix models, and are studied as discrete models of quantum gravity for arbitrary dimensions. Among them, the canonical tensor model (CTM) is a rank-three tensor model formulated as a totally constrained system with a number of first-class constraints, which have a similar algebraic structure to the constraints of the Arnowitt–Deser–Misner formalism of general relativity. In this paper, we formulate a super-extension of CTM as an attempt to incorporate fermionic degrees of freedom. The kinematical symmetry group is extended from $O(N)$ to $OSp(N, \tilde{N})$, and the constraints are constructed so that they form a first-class-constraint super-Poisson algebra. This is a straightforward super-extension, and the constraints and their algebraic structure are formally unchanged from the purely bosonic case, except for the additional signs associated with the fermionic degrees of freedom. However, this extension contains negative norm states in the quantized case, and requires some future improvements as quantum gravity with fermions. On the other hand, various results obtained so far for the purely bosonic case should have parallels in this straightforward super-extension, such as the exact physical wave functions and the connection to randomly connected tensor networks.

.....

Subject Index A64

1. Introduction

Tensor models [1–3] were introduced with the hope of analytically describing simplicial quantum gravity for arbitrary dimensions¹ by extending the matrix models that successfully describe 2D simplicial quantum gravity [6]. Subsequently, tensor models with group-valued indices [7,8], called group field theories [9–11], have been introduced, and have been extensively studied, especially in connection with loop quantum gravity. Some serious problems of the original tensor models [2,12] have been overcome by the advent of the colored tensor models [13], and various interesting concrete results on their properties have been obtained [14] (see, for instance, Refs. [15–19] for some recent developments). The colored tensor models have also stimulated the renormalization group analysis of the group field theories (see, for instance, Refs. [20–25] for some recent developments).

One of the main themes of the study of tensor models or generally in quantum gravity is to pursue the physical mechanism for generation of the classical space-time like our universe. In the tensor models above, spaces are represented by simplicial manifolds, which are generated as duals to the

¹ However, see Refs. [4,5] for a recent approach to 3D quantum gravity in terms of matrix models.

Feynman diagrams in the perturbative treatments of tensor models. The large- N analyses of the colored tensor models have shown that the generated simplicial manifolds are dominated by branched polymers [14,26,27]. Naively, the result would be an obstacle to the tensor models becoming sensible models of our space-time, since branch polymers do not seem like an extended entity in large scales. In fact, there is some interesting active research into colored tensor models to overcome this difficulty in terms of dynamically realized symmetries [15,16] and higher orders [17,28–31]. On the other hand, in causal dynamical triangulation, which is a Lorentzian model of simplicial quantum gravity, it has been shown that de Sitter-like space-times, similar to our actual universe, are generated [32]. This success can be contrasted with the unsuccessful situation in dynamical triangulation, which is the original Euclidean model. The main difference between the two models is the existence of the causal time-like direction in the former. Therefore, this success indicates the importance of a time-like direction in quantum gravity, and raises the possibility of improving the tensor models above, which basically deal with Euclidean cases, by incorporating a time-like direction.

With the motivation above, one of the present authors has formulated a tensor model in the Hamiltonian formalism (the canonical tensor model, CTM) [33–35]². It has been formulated as a totally constrained system similar to the Arnowitt–Deser–Misner (ADM) formalism of general relativity [37–41]. CTM has a close parallel with the ADM formalism in the sense that CTM contains analogues of the Hamiltonian and momentum constraints of the ADM. It is, therefore, expected to respect the central principle of general relativity; i.e., the space-time general covariance. Under some reasonable physical assumptions, the model with a canonically conjugate pair of rank-three symmetric real tensors, the minimal model, has been shown to be unique with a free real parameter [34].

The analyses so far have revealed various fascinating properties of CTM. The $N = 1$ case of CTM was shown to be equivalent to the mini-superspace approximation of general relativity, and the free parameter mentioned above has been identified with the “cosmological constant” [42]. It has been shown that there exists a formal continuum limit in which the constraint Poisson algebra of CTM agrees with that of ADM [43]. In the analysis, a correspondence between the variables of CTM and the metric tensor field of general relativity has partially been obtained [43]. It has been found that CTM and statistical systems on random networks have intimate relations: the renormalization group flows of randomly connected tensor networks can be described by the Hamiltonian of CTM [44–46]. The quantization of CTM is straightforward [47], and one can obtain a number of exact physical wave functions by explicitly solving the sets of partial differential equations representing the constraints for small N [47,48], and also by exploiting the relation between CTM and randomly connected tensor networks for general N [48]. It has been observed that the physical wave functions have singular behaviors at the configurations of potential physical importance characterized by locality [47] or Lie group symmetries [48]³. The above interesting properties of CTM obtained so far ensure that CTM is worth further study.

The main purpose of the present paper is to present an attempt to incorporate fermionic degrees of freedom into CTM. The origin of spinning particles is a deeply interesting question (for recent

² See Ref. [36] for a Hamiltonian approach in the framework of group field theories.

³ Thus, in CTM, it would be plausible that physically important configurations are stressed by physical wave functions. This is in contrast with the situation in the Euclidean rank-three tensor models, in which the actions were initially fine-tuned so that the minima generate physically sensible backgrounds [49,50].

work, see, for instance, Ref. [51] and references therein), and the most promising way to incorporate such degrees of freedom in the case of CTM is not obvious. In this paper, we make an attempt to do this in the most straightforward manner by making use of Grassmann-odd variables. We introduce odd-type indices, and assume that the tensorial variables with an odd number of odd-type indices have the Grassmann-odd property. This provides a straightforward extension of CTM in the sense that the constraints and their algebra are formally similar to the purely bosonic case, except for the additional signs associated with the order of the odd indices and variables. Thus, the kinematical symmetry is extended from $O(N)$ to $OSp(N, \tilde{N})$, and the Hamiltonian constraints form a first-class constraint algebra with the kinematical constraints for the super-extended symmetry. However, this simple extension suffers from negative norm states in the quantized case. Therefore, without some improvements in the future, this super-extension cannot be considered as a valid model of quantum gravity with fermions. On the other hand, as in the purely bosonic case [44–46], this super-extended model can be connected to the inclusion of fermionic degrees of freedom into the dual statistical systems, randomly connected tensor networks, since the connection is based on its classical properties. We would also expect that the exact physical wave functions obtained previously [47,48] can be super-extended.

The paper is organized as follows. In Sect. 2, we write down the basic definitions concerning indices and variables, paying attention to their Grassmann-even or -odd properties. In Sect. 3, we introduce some graphical representations that can describe the complications of the signs associated with ordering in simplified manners. We also present some graphical identities that are useful for the computations in the subsequent sections. In Sect. 4, we consider the super-extension of the constraints from the bosonic case, and explicitly compute the Poisson algebra among them to show that they form a first-class constraint algebra. The constraints and their algebra are essentially the same as the purely bosonic case, except for the signs. In Sect. 5, we impose the reality condition on the variables, and check the consistency. In Sect. 6, we perform the quantization of the super-extended model. This is straightforward, and the quantized constraint algebra has basically the same form as the purely bosonic case. The final section is devoted to the summary and discussions. The details of the computations in Sect. 4 are shown in the appendix.

2. Basic definitions

In this section, we introduce super-extensions of the dynamical variables and some related basic matters. The notations used here are not exactly, but largely, based on Refs. [52,53].

Let us consider that any index a of a tensor runs through a set of labels. The labels are classified by a Z_2 grade $|a| = 0$ or 1 , where the total number of even ones with $|a| = 0$ is given by N , while that of odd ones with $|a| = 1$ is by \tilde{N} . Then, each component of a variable A with p indices is assumed to have a Z_2 grade defined by

$$|A_{a_1 a_2 \dots a_p}| = \sum_{i=1}^p |a_i| \pmod{2}. \quad (1)$$

The Z_2 grades of variables determine the properties under the change of their orders, namely, their even (bosonic) or odd (fermionic) properties, as

$$\begin{aligned} A_{a_1 \dots a_p} B_{b_1 \dots b_q} &= (-1)^{|A_{a_1 \dots a_p}| |B_{b_1 \dots b_q}|} B_{b_1 \dots b_q} A_{a_1 \dots a_p} = (-1)^{\sum_{ij} |a_i| |b_j|} B_{b_1 \dots b_q} A_{a_1 \dots a_p} \\ &= (-1)^{\sum_{ij} a_i b_j} B_{b_1 \dots b_q} A_{a_1 \dots a_p}. \end{aligned} \quad (2)$$

Here, in the second line, we have given an abbreviation frequently used in this paper. Obviously,

$$(-1)^{2a} = 1, \quad (-1)^{aa} = (-1)^a \quad (3)$$

hold for an arbitrary grade $a = 0, 1$.

A totally symmetric three-index tensor, in the super-extended case, is defined by

$$M_{abc} = (-1)^{a(b+c)} M_{bca} = (-1)^{c(a+b)} M_{cab} = (-1)^{ba} M_{bac} = (-1)^{bc} M_{acb} = (-1)^{ab+bc+ca} M_{cba}, \quad (4)$$

with the additional signs coming from the grade. This symmetric condition is imposed on both the dynamical variables M, P of CTM. In the following, we will also be dealing with antisymmetric matrices, which will appear as the coefficients for the kinematical constraints. In the purely bosonic case, the kinematical constraints are the generators of the orthogonal transformations, and the coefficients are antisymmetric matrices. In the super-extended case, the antisymmetric matrices are characterized by

$$R_{ab} = -(-1)^{ab} R_{ba} \quad (5)$$

with the additional sign. Thus, the kinematical symmetry is extended to an OSp group.

At this point, we define a *constant bosonic symmetric* matrix and its inverse, denoted by Ω , satisfying

$$\begin{aligned} \Omega_{ab} &= (-1)^{ab} \Omega_{ba}, \\ \Omega^{ab} &= (-1)^{ab} \Omega^{ba}, \\ \Omega_{ab} \Omega^{bc} &= \delta_a^c, \\ \Omega_{ab} &= \Omega^{ab} = 0, \text{ if } (-1)^{a+b} = -1. \end{aligned} \quad (6)$$

Here, notice that Ω is invertible and nonsingular, which also means that \tilde{N} must be even. The last condition in (6), which requires Ω to be bosonic, may not be necessary in general, but we assume it for the simplicity of the index contractions defined below. Ω defines the relations between the variables with lower and upper indices as

$$A^a = A_b \Omega^{ba}, \quad A_a = A^b \Omega_{ba}, \quad (7)$$

and similarly for matrices and tensors. Thus, in the formalism developed here, Ω plays the role of a metric for index contractions.

The commutator of matrices will be defined in the usual manner and is given by

$$[A, B]_{ab} = A_a{}^c B_{cb} - B_a{}^c A_{cb}. \quad (8)$$

Following the standard procedure, the fundamental Poisson bracket is defined by

$$\begin{aligned} \{M_{abc}, P^{def}\} &= -\{P_{abc}, M^{def}\} = \delta_{abc}^{fed}, \\ \{M_{abc}, M^{def}\} &= \{P_{abc}, P^{def}\} = 0, \end{aligned} \quad (9)$$

where

$$\begin{aligned} \delta_{abc}^{fed} &\equiv \delta_a^f \delta_b^e \delta_c^d + (-1)^{f(e+d)} \delta_a^e \delta_b^d \delta_c^f + (-1)^{d(f+e)} \delta_a^d \delta_b^f \delta_c^e + (-1)^{ef} \delta_a^e \delta_b^f \delta_c^d \\ &+ (-1)^{de} \delta_a^f \delta_b^d \delta_c^e + (-1)^{de+ef+fd} \delta_a^d \delta_b^e \delta_c^f. \end{aligned} \quad (10)$$

Here the signs are necessarily imposed in order to be consistent with the symmetric condition written in (4); note also that the orders of the upper indices def on M, P are reversed in the rightmost expression in (9). To define the Poisson bracket for general cases, let us start by introducing the following right and left first-order partial derivatives with respect to M, P , which satisfy

$$\begin{aligned} \vec{D}_{abc}^M M^{def} &= \vec{D}_{abc}^P P^{def} = \delta_{abc}^{fed}, \\ M_{abc} \overleftarrow{D}_M^{def} &= P_{abc} \overleftarrow{D}_P^{def} = \delta_{abc}^{fed}. \end{aligned} \tag{11}$$

These are not simple partial derivatives due to the symmetric factors implicitly contained in (10)⁴. One also has to be careful with the order of indices, which can introduce an additional sign in the computation. The partial derivatives are assumed to satisfy the following Leibniz rule:

$$\begin{aligned} \vec{D}_{abc}^M (AB) &= \left(\vec{D}_{abc}^M A \right) B + (-1)^{|A|(a+b+c)} A \left(\vec{D}_{abc}^M B \right), \\ (AB) \overleftarrow{D}_M^{abc} &= A \left(B \overleftarrow{D}_M^{abc} \right) + (-1)^{|B|(a+b+c)} \left(A \overleftarrow{D}_M^{abc} \right) B, \end{aligned} \tag{12}$$

and the same for D^P, D_P . This is a sort of generalization of the usual Leibniz rule, taking into account the grade of the tensor indices. Then, using this, one can easily define the super-Poisson bracket for general cases by

$$\{A, B\} = \frac{1}{6} \left[\left(A \overleftarrow{D}_M^{abc} \right) \left(\vec{D}_{cba}^P B \right) - \left(A \overleftarrow{D}_P^{abc} \right) \left(\vec{D}_{cba}^M B \right) \right]. \tag{13}$$

This indeed reproduces the fundamental Poisson bracket written in (9) by making use of the identity $\delta_{abc}^{ihg} \delta_{ihg}^{fed} = 6\delta_{abc}^{fed}$. This super-Poisson bracket has the following anticommutative property:

$$\{A, B\} = -(-1)^{|A||B|} \{B, A\}. \tag{14}$$

From the Leibniz rule (12), one can also derive the Leibniz rule for the Poisson bracket:

$$\begin{aligned} \{AB, C\} &= A \{B, C\} + (-1)^{|B||C|} \{A, C\} B, \\ \{A, BC\} &= \{A, B\} C + (-1)^{|A||B|} B \{A, C\}. \end{aligned} \tag{15}$$

The Poisson bracket also satisfies the Jacobi identity:

$$\{\{A, B\}, C\} = \{A, \{B, C\}\} + (-1)^{BC} \{\{A, C\}, B\}. \tag{16}$$

3. Graphical representation and identities

The number of indices with grades involved in the tensorial computation is large. This easily exponentiates the complexity in the manipulation and handling of the algebra, and therefore demands a methodology to simplify this task. This will be achieved by making use of graphs to do index contractions and recognize the signs graphically.

The most basic expression can be written in a diagrammatic form as

$$A^a B_a : A \dashrightarrow B. \tag{17}$$

⁴ For instance, for the case $a = b = c = d = e = f = \text{even}$, (10) produces a factor of 6, and (11) differs by this factor from the usual partial derivatives. This factor necessarily appears for the compatibility between (4) and the kinematical symmetry.

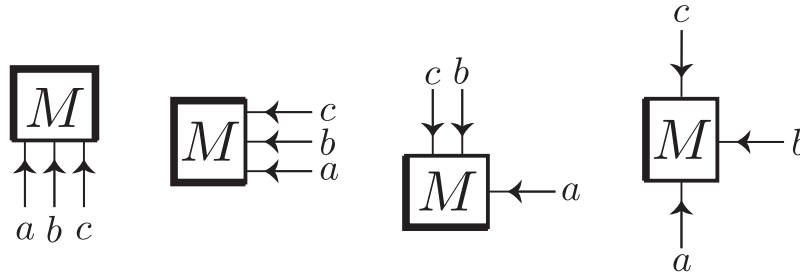


Fig. 1. Graphical representations of M_{abc} , which are supposed to be equivalent. Here vacant edges are drawn in thick bold lines to clarify the definition. Reading off the indices on a particular box is always done in a counterclockwise manner.

$$\begin{array}{c} \diagup \\ \diagdown \\ a \quad b \end{array} = (-1)^{ab} \begin{array}{c} \uparrow \\ \uparrow \\ a \quad b \end{array}$$

Fig. 2. The sign associated with a crossing.

The generalization for multiple indices and variables can be done systematically. Firstly, we introduce the following requirements:

- (I) In a graph, variables are ordered in a horizontal direction, in the same order as they appear in a formula.
- (II) A contracted pair of indices are connected by an arrow that starts from an upper index and ends on a lower one.

Here, the requirements stated in (I) and (II), respectively, come from the dependence of overall signs on both the order of variables as in (2) and the two methods of contraction as

$$A^a B_a = (-1)^a B_a A^a = (-1)^a A_a B^a. \tag{18}$$

We introduce a box to represent a variable, rather than using the bare expression as in (17) for a vector. For instance, a three-index tensor M_{abc} is represented as in Fig. 1, where all the graphs are supposed to be equivalent. In general, the correspondence between a multi-index variable and a graph is defined by the following rules:

- (III) A variable is represented by a box containing its label.
- (IV) Indices of a variable are assigned counterclockwise on arrows attached to a box.
- (V) The first index of a variable is assigned to the arrow that appears first after the vacant edges of a box in a counterclockwise direction. Here, vacant edges mean those with no arrows attached; they must form a connected bunch for well-definedness (see Fig. 1).

It is convenient to associate a sign with a crossing of two lines, as in Fig. 2. A merit of this convention is to simplify the symmetric condition (4): signs coming from reordering of indices of a symmetric tensor can be represented by crossings, as in Fig. 3. The convention also simplifies the antisymmetric condition (5), as in Fig. 4. We also have a graphical identity, Fig. 5, corresponding to the last equation of (18).

A very convenient graphical identity that will be used frequently in later computations is shown in Fig. 6. This identity allows one to change the order of variables. The identity for the simplest case of

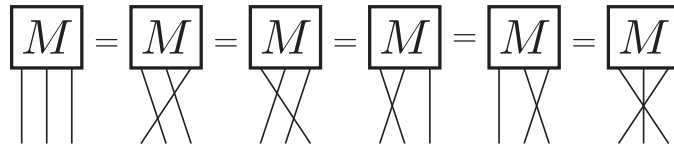


Fig. 3. The symmetric condition (4) in terms of graphs. This holds for P as well.

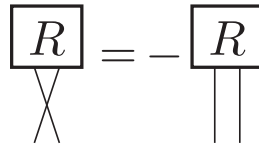


Fig. 4. The antisymmetric condition (5) in terms of graphs.

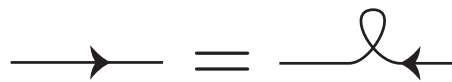


Fig. 5. The identity to reverse an orientation of an arrow corresponding to the last equation of (18). The sign is represented by the self-crossing due to $(-1)^{aa} = (-1)^a$.

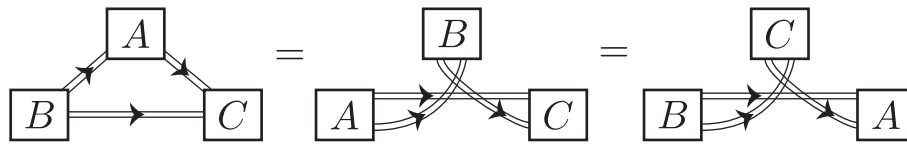


Fig. 6. An identity for reordering variables. In the above figure, A, B, C , and the double-line arrows represent bunches of variables and arrows, respectively. The identity still holds, even when some of A, B, C , or the double-line arrows are absent, when bunches of arrows contain antiparallel arrows, and when arrows cross in other ways. The essential points are (i) before and after reordering, the connections and directions of arrows must be kept, except for those connecting reordered variables; and (ii) as for the arrows connecting reordered variables, they must be reconnected with reversed directions in the ways shown in the figure.

the first equality can be proven by

$$\begin{aligned}
 A^{ab} B_b^c &= (-1)^{(a+b)(b+c)} B_b^c A^{ab} \\
 &= (-1)^{(a+b)(b+c)+b} B^{bc} A^a_b \\
 &= (-1)^{ab+bc+ca} B^{bc} A^a_b,
 \end{aligned}
 \tag{19}$$

where we have used $|A^{ab}| = |a| + |b|$, $|B_b^c| = |b| + |c| \pmod 2$ for (2) and (18) for the index b . Here, the nice thing is that the cumbersome sign in the last line of (19) is accounted for graphically by the crossings of the arrows. The proof can obviously be generalized to other cases. In fact, the identity shown in Fig. 6 is a representative of various variants of the identity: some of A, B, C , or the double-line arrows may be absent, double-line arrows may contain antiparallel arrows, and there may exist other crossings of arrows. To illustrate this, two of such variants are shown in Fig. 7. Basically, all the computations in the following sections can be performed by mostly using the variants of the identity and the basic properties of the variables.

Finally, we will show the graphical representation of the fundamental Poisson bracket. By using the Leibniz rule (15), the computation of a Poisson bracket between arbitrary quantities can be reduced

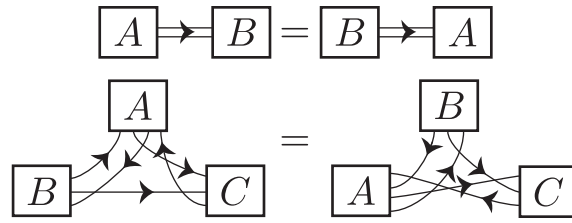


Fig. 7. Two examples of variants of the identity shown in Fig. 6.

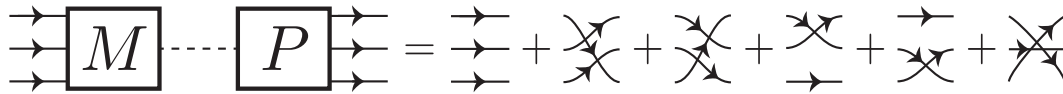


Fig. 8. The graphical representation of the fundamental Poisson bracket (9). It is given by the summation of the six graphs in the figure. The dashed line indicates the pair between which the fundamental Poisson bracket is taken. The cumbersome signs in (9) are represented by the sign assignment of Fig. 2 to the crossings.

to the summation of terms containing only the fundamental Poisson bracket. The graphical representation of the fundamental Poisson bracket is given in Fig. 8. In the figure, we use a dashed line to indicate a pair of M, P , between which the fundamental Poisson bracket is taken. An advantage of this graphical representation is that the cumbersome signs appearing in (9) can be represented by the crossings due to the sign assignment shown in Fig. 2.

4. The Poisson algebra of the constraints

In this section, we define the constraints in the super-extended case, and show the Poisson algebra satisfied by them. It turns out that the constraints, as well as the constraint Poisson algebra, are formally unchanged from the purely bosonic case, in the sense that the overall structure of the constraints and the algebra satisfied by them is very similar (modulo signs). This formal simplicity is due to the validity and consistency of the basic properties imposed on the parameters and dynamical variables in the previous sections.

By simply transferring the purely bosonic case to the present super-extended case by taking care with index orderings, we consider the Hamiltonian constraints defined by

$$\mathcal{H}_a = \frac{1}{2} \left(P_a^{bc} P_c^{de} M_{edb} - \lambda M_a^b{}_b \right), \tag{20}$$

where λ is a real constant. It was shown in the purely bosonic case that λ can be interpreted as a cosmological constant, because the $N = 1$ case in CTM exactly reproduces the mini-superspace approximation of general relativity with a cosmological constant proportional to λ [42]. For this reason, we also call λ the cosmological constant in the present case.

It is convenient at this point to introduce a nondynamical variable T^a , and consider

$$H(T) = T^a \mathcal{H}_a = \frac{1}{2} \left(T^a P_a^{bc} P_c^{de} M_{edb} - \lambda T^a M_a^b{}_b \right). \tag{21}$$

For convenience, we consider the two terms separately by defining $H_0(T) = H(T)|_{\lambda=0}$. Similarly, the momentum constraints are given by

$$J(R) = -\frac{1}{2} R^{ab} P_b^{cd} M_{dca}, \tag{22}$$

where R is a nondynamical matrix variable with the antisymmetric property (5), and the overall minus sign is for convenience. The graphical representations of the constraints are depicted diagrammatically in Fig. 9 up to the numerical factors.

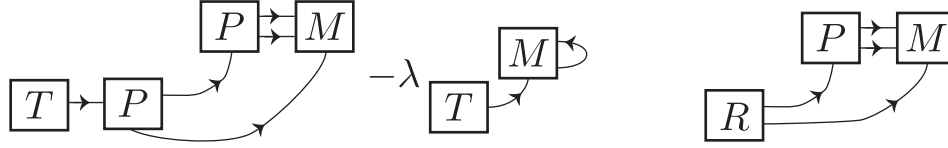


Fig. 9. The graphical representations of $H(T)$ in (21) and $J(R)$ in (22) are given by the left and right figures, respectively, up to the numerical factors.

The constraint algebra is worked out explicitly by using the diagrammatic notation in Appendix A. The result is that the constraints form a set of first-class constraints, satisfying the following first-class Poisson algebra:

$$\{H(T_1), H(T_2)\} = J\left([\tilde{T}_1, \tilde{T}_2] + 2\lambda T_1 \wedge T_2\right), \tag{23}$$

$$\{H(T), J(R)\} = H(TR), \tag{24}$$

$$\{J(R_1), J(R_2)\} = J([R_1, R_2]), \tag{25}$$

where the matrix commutator is defined in (8), and $\tilde{T}_{ab} = T^c P_{cab}$, $(T_1 \wedge T_2)^{ab} = T_1^a T_2^b - T_2^a T_1^b$, and $(TR)_a = T^b R_{ba}$.

The consistency that the arguments of J be antisymmetric on the right-hand sides of (23) and (25) can be checked from

$$\begin{aligned} (\tilde{T}_1 \tilde{T}_2)^{ab} &= T_1^c P_c^{ad} T_2^e P_{ed}^b = (-1)^{(d+b)(a+d)+bd+ad+d} T_2^e P_e^{bd} T_1^c P_{cd}^a = (-1)^{ab} (\tilde{T}_2 \tilde{T}_1)^{ba}, \\ (R_1 R_2)^{ab} &= R_1^{ac} R_{2c}^b = (-1)^{(a+c)(b+c)+ac+bc+c} R_2^{bc} R_{1c}^a = (-1)^{ab} (R_2 R_1)^{ba}. \end{aligned} \tag{26}$$

In the case of $\lambda = 0$, one can add another constraint given by

$$D = \frac{1}{6} P^{abc} M_{cba}. \tag{27}$$

This satisfies $\{D, P_{abc}\} = P_{abc}$, $\{D, M_{abc}\} = -M_{abc}$, and D is therefore a dilatational constraint. Such a dilatational constraint plays a vital role in the connection between CTM and statistical systems on random networks; i.e., randomly connected tensor networks [44–46]. From the dilatational property of D , it is obvious that D forms a first-class constraint algebra with H_0 and J as

$$\{D, H_0(T)\} = H_0(T), \tag{28}$$

$$\{D, J(R)\} = 0. \tag{29}$$

5. Reality condition

The minimal set of dynamical variables of the purely bosonic CTM consists of a canonically conjugate pair of rank-three real symmetric tensors M, P . To consider this minimal setting in the super-extended case, we will impose reality conditions on the super-extended variables in this section. We will also check the consistency of the reality conditions with the constraints.

We denote the complex conjugation of a variable A by A^* , and require that⁵

$$(A_1 A_2 \dots A_n)^* = A_n^* A_{n-1}^* \dots A_1^* \quad (30)$$

for the complex conjugate of a product of variables A_i . We consider Ω to be real for even index values, and pure imaginary for odd ones, respectively (note that, from the definition (6), Ω does not have Grassmann-odd components). From this demand, we obtain the complex conjugate of the Ω :

$$\begin{aligned} \Omega_{ab}^* &= (-1)^{ab} \Omega_{ab} = \Omega_{ba}, \\ \Omega^{ab*} &= (-1)^{ab} \Omega^{ab} = \Omega^{ba}, \end{aligned} \quad (31)$$

where (6) should also be remembered. It is important to notice that the complex conjugation is generally not commutative with raising and lowering indices. This can be seen by

$$(A_a)^* = (A^b \Omega_{ba})^* = \Omega_{ab} A^{b*} \neq A^{b*} \Omega_{ba} \quad (32)$$

in general. Therefore, the definition of the complex conjugation of A depends on whether it is defined by upper or lower components. We also obtain

$$(A^a B_a)^* = (A_a \Omega^{ab} B_b)^* = B_b^* \Omega^{ba} A_a^* = B^{*a} A_a^*. \quad (33)$$

Graphically, this is

$$(A \rightarrow B)^* = B^* \rightarrow A^*; \quad (34)$$

namely, the complex conjugation is a reflection in the horizontal direction, but with reversed connections of arrows. Here, as mentioned above, it is important to define the complex conjugations of variables for fixed positions (upper or lower) of their indices. Thus, throughout this paper, we define the complex conjugation of tensors (vectors and matrices as well) by their lower components. For example, $A^*_a = A_a^*$, and $A^{*a} = A_b^* \Omega^{ba}$, as used in (33). One could define the complex conjugation of a variable by its upper components as well, but mixtures of the two methods of definition would lead to unnecessary complications.

From the reflection property (34) of the complex conjugation, it is natural to define the reality/imaginary condition in the case of tensors to be the one dictating its relation with the tensor with reversed indices:

$$T_{a_1 a_2 \dots a_p}^* = \pm T_{a_p a_{p-1} \dots a_1}. \quad (35)$$

This is indeed what was imposed on Ω in (31) with a plus sign. We impose the reality conditions on the dynamical variables as

$$\begin{aligned} M_{abc}^* &= M_{cba}, \\ P_{abc}^* &= P_{cba}. \end{aligned} \quad (36)$$

The reality conditions on the nondynamical variables are given by

$$\begin{aligned} T_a^* &= T_a, \\ R_{ab}^* &= -R_{ba} = (-1)^{ab} R_{ab}, \end{aligned} \quad (37)$$

where (5) should also be remembered. Because of the antisymmetry (5) of R , we have to consider the reality condition with a minus sign in (37) to recover the usual reality condition in the purely bosonic case.

⁵ We follow Ref. [52] for the convention.

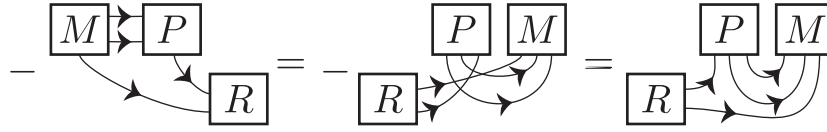


Fig. 10. The proof of reality for $J(R)$.

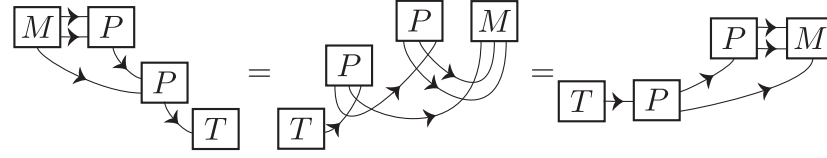


Fig. 11. The proof of reality for $H_0(T)$.

The proof of the reality of the constraints is straightforward. The proof for $J(R)$ is shown in Fig. 10. The first graph is obtained from that for $J(R)$ in Fig. 9 by taking its reflection with reversed arrows, and its minus sign comes from (37). The second one is obtained by using variants of the reordering identity, Fig. 6. Finally, the third one is obtained by the symmetric/antisymmetric properties of the variables, Figs. 3 and 4. The proof of reality for $H_0(T)$ proceeds basically along the same lines, as shown in Fig. 11. It is also easy to show the reality of the cosmological constant term in (21), and the dilatational constraint (27).

Finally, we should check whether the reality conditions are satisfied for the arguments of the constraints on the right-hand sides of the constraint algebra (23), (24), and (25):

$$\begin{aligned}
 (\tilde{T}_1 \tilde{T}_2)_{ab}^* &= (T_1^c P_{ca}{}^d T_2^e P_{edb})^* = P_b{}^{de} T_{2e} P_{da}{}^c T_{1c} = (-1)^{ab} T_1^c P_{ca}{}^d T_2^e P_{edb} = (-1)^{ab} (\tilde{T}_1 \tilde{T}_2)_{ab}, \\
 (T_{1a} T_{2b})^* &= T_{2b} T_{1a} = (-1)^{ab} T_{1a} T_{2b}, \\
 (TR)_a^* &= (T^b R_{ba})^* = -R_a{}^b T_b = T^b R_{ba}, \\
 (R_1 R_2)_{ab}^* &= (R_{1a}{}^c R_{2cb})^* = R_{2b}{}^c R_{1ca} = (-1)^{ab} R_{1a}{}^c R_{2cb} = (R_1 R_2)_{ab},
 \end{aligned}
 \tag{38}$$

where we have used (36), (37), and (33) concerning the complex conjugation, and have reordered the variables and indices with attention to the signs using (2), (4), (5), and (18).

6. Quantization

In this section, we carry out the quantization of the classical system discussed so far. The quantized operator corresponding to a classical quantity A will be denoted by \hat{A} , and the same Z_2 grade will be assigned; i.e., $|\hat{A}| = |A|$. We assume the same symmetric properties (4) for the quantized dynamical variables \hat{M} , \hat{P} . As for the reality condition, we impose

$$\begin{aligned}
 \hat{M}_{abc}^\dagger &= \hat{M}_{cba}, \\
 \hat{P}_{abc}^\dagger &= \hat{P}_{cba},
 \end{aligned}
 \tag{39}$$

similar to (36), where \hat{A}^\dagger denotes the Hermitian conjugate of \hat{A} . A reflection property similar to (33) holds, since

$$(\hat{f}^a \hat{g}_a)^\dagger = (\hat{f}_a \Omega^{ab} \hat{g}_b)^\dagger = \hat{g}_b^\dagger (\Omega^{ab})^* \hat{f}_a^\dagger = \hat{g}_b^\dagger \Omega^{ba} \hat{f}_a^\dagger = \hat{g}^{\dagger a} \hat{f}_a^\dagger,
 \tag{40}$$

where we should note that $(\hat{g}^a)^\dagger \neq \hat{g}^{\dagger a}$ in general, if \hat{g}^\dagger is defined through its lower components. The definition of the Hermitian conjugate with lower components is assumed throughout this paper, as the complex conjugation in Sect. 5.

The fundamental commutator is defined by

$$\begin{aligned} [\hat{M}_{abc}, \hat{P}^{def}] &= -[\hat{P}_{abc}, \hat{M}^{def}] = i \delta_{abc}^{fed}, \\ [\hat{M}_{abc}, \hat{M}^{def}] &= [\hat{P}_{abc}, \hat{P}^{def}] = 0, \end{aligned} \quad (41)$$

where $[\ , \]$ is the operator commutator

$$[\hat{A}, \hat{B}] = \hat{A}\hat{B} - (-1)^{|\hat{A}||\hat{B}|} \hat{B}\hat{A}. \quad (42)$$

The commutator satisfies

$$[\hat{A}, \hat{B}] = -(-1)^{|\hat{A}||\hat{B}|} [\hat{B}, \hat{A}]. \quad (43)$$

By assuming the associativity of the products of operators, one can readily prove the Leibniz rule:

$$\begin{aligned} [\hat{A}\hat{B}, \hat{C}] &= \hat{A}[\hat{B}, \hat{C}] + (-1)^{|\hat{B}||\hat{C}|} [\hat{A}, \hat{C}]\hat{B}, \\ [\hat{A}, \hat{B}\hat{C}] &= [\hat{A}, \hat{B}]\hat{C} + (-1)^{|\hat{A}||\hat{B}|} \hat{B}[\hat{A}, \hat{C}], \end{aligned} \quad (44)$$

and the Jacobi identity in the operator language:

$$[[\hat{A}, \hat{B}], \hat{C}] = [\hat{A}, [\hat{B}, \hat{C}]] + (-1)^{|\hat{B}||\hat{C}|} [[\hat{A}, \hat{C}], \hat{B}] \quad (45)$$

Note that the Leibniz rules (44) have the same form as the classical ones (15). This means that the computation of the commutation algebra of the quantized constraints proceeds in exactly the same manner as the classical case⁶, if the orders of \hat{M} , \hat{P} are not changed during the computation, since the classical Poisson algebra (23), (24), (25), (28), and (29) of the constraints can in principle be derived solely by using (9) and (15). As will be discussed in due course, this fact will ensure that the classical Poisson algebra can be translated without any essential modifications to a quantum commutation algebra.

As the reality condition on the classical constraints, we impose hermiticity on the quantized constraints. By replacing the variables in (21), (22) and (27) with the quantized ones and taking into account the possible normal ordering term, the hermiticity condition determines the quantized Hamiltonian, momentum and dilatational constraints as

$$\hat{H}(T) = \frac{1}{2} T^a \left(\hat{P}_a^{bc} \hat{P}_c^{de} \hat{M}_{edb} + i \lambda_H \hat{P}_a^b \hat{P}_b - \lambda \hat{M}_a^b \hat{P}_b \right), \quad (46)$$

$$\hat{J}(R) = -\frac{1}{2} R^{ab} \hat{P}_b^{cd} \hat{M}_{dca}, \quad (47)$$

$$\hat{D} = \frac{1}{6} \left(\hat{P}^{abc} \hat{M}_{cba} + i \lambda_D \right), \quad (48)$$

where λ_H, λ_D are real constants coming from the normal ordering, and will be determined below. As will be checked below, there are no normal ordering terms for $\hat{J}(R)$.

⁶ Except of course for the prefactor i in (41).

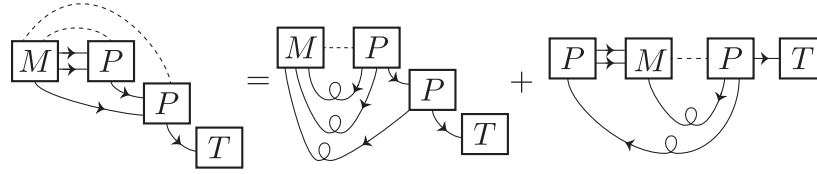


Fig. 12. Computation of the normal ordering term in $\hat{H}(T)$. The dashed lines indicate the pairs of \hat{M}, \hat{P} , between which the fundamental commutators are taken.



Fig. 13. By substituting the fundamental commutator into Fig. 12, one obtains some graphs containing the elementary ones shown in the figure.

Let us first check the hermiticity of $\hat{J}(R)$. By taking the Hermitian conjugate, we obtain

$$\begin{aligned} \hat{J}(R)^\dagger &= -\frac{1}{2} \hat{M}^{acd} \hat{P}_{dc}{}^b R_{ba} \\ &= \hat{J}(R) - \frac{1}{2} [\hat{M}^{acd}, \hat{P}_{dc}{}^b] R_{ba}, \end{aligned} \tag{49}$$

where we have used (37), (39), and (40). From (41), it is obvious that the second term can only produce either $R_{ab} \Omega^{ba}$ or $(-1)^a R_{ab} \Omega^{ba} = R_{ab} \Omega^{ab}$, which both vanish due to the symmetry/antisymmetry properties of R, Ω . Therefore, (47) is Hermitian.

To study the hermiticity of the quantized Hamiltonian constraint, let us take the Hermitian conjugate of the first term of (46). Similarly to the above, we obtain

$$\left(T^a \hat{P}_a{}^{bc} \hat{P}_c{}^{de} \hat{M}_{edb} \right)^\dagger = \hat{M}^{bde} \hat{P}_{ed}{}^c \hat{P}_{cb}{}^a T_a = T^a \hat{P}_a{}^{bc} \hat{P}_c{}^{de} \hat{M}_{edb} + (\text{Fig. 12}), \tag{50}$$

where the normal ordering terms are shown in Fig. 12. Here, we have used some variants of the identity stated in Fig. 6, and have also reversed the orientations of some of the arrows by using the rule given in Fig. 5. By making use of Fig. 8, we obtain a sum of graphs that contain the elementary ones shown in Fig. 13. The left graph produces a numerical factor $\sum_a (-1)^a = N - \tilde{N}$, and the right $(-1)^{2a} \delta_a^b = \delta_a^b$. By summing over all the contributions, we obtain

$$(\text{Fig. 12}) = (N - \tilde{N} + 2) (N - \tilde{N} + 3) T^a P_a{}^b{}_b. \tag{51}$$

Therefore, the hermiticity of $\hat{H}(T)$ is obtained by putting⁷

$$\lambda_H = \frac{1}{2} (N - \tilde{N} + 2) (N - \tilde{N} + 3). \tag{52}$$

One can see in this expression that the fermionic degrees of freedom contribute in an opposite manner to the bosonic ones, as commonly argued. In the same manner, we obtain

$$\lambda_D = \frac{1}{2} (N - \tilde{N}) (N - \tilde{N} + 1) (N - \tilde{N} + 2). \tag{53}$$

As discussed above, the computation of the commutation algebra of the quantized constraints is basically the same as the classical one, if we keep the ordering of \hat{M}, \hat{P} , because of the formal

⁷ The apparent difference by 6 of the numerical factors of $\lambda_{H,D}$ from those in Ref. [48] comes from the different normalization of the fundamental commutator (41).

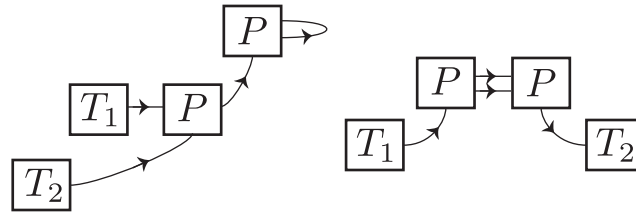


Fig. 14. The terms generated from the commutator $[T_1^a \hat{P}_a^{bc} \hat{P}_c^{de} \hat{M}_{edb}, T_2^a \hat{P}_a^{b}]$.

equivalence between the identities satisfied by the Poisson bracket and the commutator. We take the normal ordering that \hat{M} be always the rightmost if it exists, as in the expressions of $\hat{H}(T)$, $\hat{J}(R)$, \hat{D} in (46), (47), (48), respectively. Under this convention of ordering, the same part of the quantized constraints as the classical ones generates the same algebra as the classical case. The only difference between the quantum and classical constraints is the existence of the normal ordering term proportional to $\hat{P}_a^{b_b}$ in \hat{H} in (46). As we will see below, this extra term does not change the commutation algebra. In Fig. 14, we show the graphs that are produced from the commutator with \hat{H}_0 , namely, $[T_1^a \hat{P}_a^{bc} \hat{P}_c^{de} \hat{M}_{edb}, T_2^a \hat{P}_a^{b_b}]$. All the terms in Fig. 14 are symmetric under $T_1 \leftrightarrow T_2$, and therefore cancel out in the computation of $[\hat{H}(T_1), \hat{H}(T_2)]$. Moreover, the normal ordering term does not cause problems with the cosmological constant term either, since the commutator between them can only produce terms of $T_1^a T_{2a}$ or $T_1^a T_{2a}(-1)^a$ type, which are symmetric under $T_1 \leftrightarrow T_2$. One can also check the covariant property of the normal ordering term with $\hat{J}(R)$, and the commutator with \hat{D} . Thus, we finally obtain the following quantum constraint commutation algebra, which is basically the same as the classical one:

$$[\hat{H}(T_1), \hat{H}(T_2)] = \hat{J}([\hat{T}_1, \hat{T}_2] + 2\lambda T_1 \wedge T_2), \tag{54}$$

$$[\hat{H}(T), \hat{J}(R)] = \hat{H}(TR), \tag{55}$$

$$[\hat{J}(R_1), \hat{J}(R_2)] = \hat{J}([R_1, R_2]), \tag{56}$$

$$[\hat{D}, \hat{H}_0(T)] = \hat{H}_0(T), \tag{57}$$

$$[\hat{D}, \hat{J}(R)] = 0, \tag{58}$$

where $\hat{T}_{ab} = T^c \hat{P}_{cab}$, and $\hat{H}_0(T) = \hat{H}(T)|_{\lambda=0}$. Here, note that the argument of \hat{J} on the right-hand side of (54) contains \hat{P} , and therefore is not commutative with the operator part of \hat{J} . Hence, we have to carefully put the argument at the leftmost position as R in the definition (47). As in the bosonic case, the commutation algebra is indeed first class, and therefore the quantization is consistent.

7. Summary and discussions

In this paper, we have made an attempt to include fermionic degrees of freedom in CTM, which initially was purely bosonic in nature. We have introduced such degrees of freedom by allowing the dynamical rank-three tensors to be either Grassmann even or odd in accordance with the Grassmann natures associated with the indices. This provides a straightforward super-extension of CTM, whose constraints and constraint algebra have basically the same form as the purely bosonic case except for the signs associated with the order of the indices and variables, extending the kinematical symmetry from $O(N)$ to $OSp(N, \tilde{N})$. To prove that the super-extended constraints form a first-class constraint

algebra, we have performed explicit computations of the super-Poisson brackets. This process was facilitated by the graphical expressions that can represent the signs associated with the ordering in a simplified manner. Then, we finally considered the quantization of the super-extended system. It has been shown that, as in the purely bosonic case, the quantized constraint algebra is formally the same as the classical one, which also means that the quantization is consistent. The quantized Hamiltonian constraint contains the normal ordering term, whose coefficient depends only on $N - \tilde{N}$, showing the opposite contributions of the bosonic and fermionic degrees of freedom.

The formalism presented in this paper obviously contains the issue of negative norm states in the quantized case⁸. This issue comes from the Grassmann-odd variables. From (41) and some basic definitions, one can see that the Grassmann-odd variables can be recast into the pairs $\psi^i, \tilde{\psi}^i$, which are Hermitian, $\psi^i = \psi^{i\dagger}, \tilde{\psi}^i = \tilde{\psi}^{i\dagger}$, and satisfy the anticommutation relations, $[\psi^i, \tilde{\psi}^j]_+ = \delta^{ij}$, $[\psi^i, \psi^j]_+ = [\tilde{\psi}^i, \tilde{\psi}^j]_+ = 0$. Then, one can consider recombinations, $\psi^i_{\pm} = \psi^i \pm \tilde{\psi}^i$, and obtain $[\psi^i_-, \psi^j_-]_+ = -2\delta^{ij}$. Since ψ^i_- is Hermitian and satisfies the last anticommutation relation, there exist negative norm states in the Hilbert space.

In order to resolve the issue in the quantized case, some directions for further study can be considered. One would be to add constraints like $\psi^i - \tilde{\psi}^i = 0$, which incorporate the fact that the fermionic degrees of freedom should be treated in a first-order Lagrangian. This would require a careful analysis of the full consistency with the original constraints. Another more physically attractive direction would be to pursue the possibility of obtaining fermionic degrees of freedom from quantization of bosonic degrees of freedom without initially introducing Grassmann-odd variables (see, for instance, Ref. [51] for a recent discussion in such a direction). It would be fascinating if the degrees of freedom of the purely bosonic CTM turned out to generate fermionic ones after quantization. Since fermionic degrees of freedom would be expected to appear as fluctuations around bosonic backgrounds, this would require some analysis of the behavior of the physical wave functions [48] in the vicinity of their peaks. Due to the spin-statistics theorem, it would even be possible that the above two different routes for resolution would finally lead to the same result.

Leaving aside the issue in the quantized case, we would like to stress that the super-extended model presented in this paper itself would have some theoretical interests of its own. One is that, because of its formal equivalence to the purely bosonic case, it would be straightforward to super-extend the results obtained so far for the purely bosonic case. This would include the exact physical wave functions [47,48] and the connection with the dual statistical systems; i.e., the randomly connected tensor networks [44–46]. In particular, since the connection of the latter is based on the classical aspects of CTM, the physical interpretations of the extension would be more solid. Although the additional degrees of freedom would not be real fermions, the super-extensions would provide general hints about how the anticommuting degrees of freedom would change the physical outcomes compared with the purely bosonic case.

Acknowledgements

G.N. would like to thank N.S. for supporting his visit to YITP, where this work was started. G.N. would like to thank his hosts, Prof. K. S. Narain and Prof. H. Nicolai, for providing support and hospitality during his stay at ICTP and the Max Planck Institute for Gravitational Physics (AEI), Golm, respectively, where part of the work was done. N.S. would like to thank Daniele Oriti for the hospitality and support during his stay in the

⁸ More details of this general aspect are explained in Ref. [53].

latter institute. We are grateful to Yuki Sato for several useful discussions during the course of this work. The work of N.S. was supported in part by JSPS KAKENHI Grant Number 15K05050.

Funding

Open Access funding: SCOAP³.

Appendix A. Poisson algebra of the constraints

In this appendix, we will prove the Poisson algebra, (23), (24), and (25), by explicit computations using the graphs introduced in Sect. 3.

A.1. Computation of $\{J, J\}$

In this subsection, we will compute $\{J(R_1), J(R_2)\}$. The computation of the Poisson bracket between $R_i^{ab} P_b^{cd} M_{dca}$ ($i = 1, 2$) is shown in Fig. A1. In the first graph, we have moved R_2 to the rightmost position by using a variant of the identity in Fig. 6 with two variables⁹, and have indicated by dashed lines the two cases of the fundamental Poisson bracket being taken. As shown in the second graph, one can easily find that the two cases contribute in opposite signs with $R_1 \leftrightarrow R_2$. By substituting the fundamental Poisson bracket (Fig. 8) into it and considering the symmetry (Fig. 3) of P, M , we obtain the last line. In fact, the second graph of the last line is symmetric under $R_1 \leftrightarrow R_2$ and cancels out. The proof of the symmetric property of the second graph is shown in Fig. A2. We therefore finally obtain the result in Fig. A3, where the first graph is obtained from the first one in the last line of Fig. A1 by moving R_2 to the leftmost position with the use of a variant of the identity in Fig. 6. By taking the sign and the normalization in (22) into account, we obtain (25).

A.2. Computation of $\{H_0, H_0\}$

In this subsection, we consider the $\lambda = 0$ case first; we will deal with the $\lambda \neq 0$ case in Appendix A.4. As shown in Fig. A4, the Poisson bracket between $T_i^a P_a^{bc} P_c^{de} M_{edb}$ ($i = 1, 2$) is given by the summation of the contributions (i) and (ii) minus the same ones with $T_1 \leftrightarrow T_2$. In comparison with Fig. A1, the computation of (i) minus its $T_1 \leftrightarrow T_2$ is basically the same as the computation of $\{J, J\}$ with the replacement $(R_i)_{ab} \rightarrow (\tilde{T}_i)_{ab} = T_i^c P_{cab}$. Therefore, after taking the sign and the normalization into account, we obtain the right-hand side of (23) with $\lambda = 0$. Thus, what remains to be shown is that the contribution (ii) cancels out with its $T_1 \leftrightarrow T_2$. In Fig. A5, the computation of the contribution (ii) is shown. In the first line, T_2 is moved to the rightmost position by using a variant of the identity in Fig. 6, and then the fundamental Poisson bracket (Fig. 8) is substituted to obtain the second line. From the second to the last line, we use some variants of Figs. 6 and 3 to deform each diagram, as shown in Fig. A6. As shown in Fig. A7, the first graph is invariant by itself under $T_1 \leftrightarrow T_2$, and the sum of the last two graphs in Fig. A6 is obviously so, too. Therefore, the contribution (ii) cancels out with its $T_1 \leftrightarrow T_2$.

A.3. Computation of $\{H_0, J\}$

In the computation of $\{H_0(T), J(R)\}$, there exist three cases of the fundamental Poisson bracket to be taken, as shown in Fig. A8. The contributions (ii) and (iii) are the same as those appearing in the computation of $\{J, J\}$ in Fig. A1, if we perform the replacement $R_1 \rightarrow \tilde{T}$, $R_2 \rightarrow R$. Thus the

⁹ Here, $P_a^{cd} M_{dcb}$ is regarded as one variable.

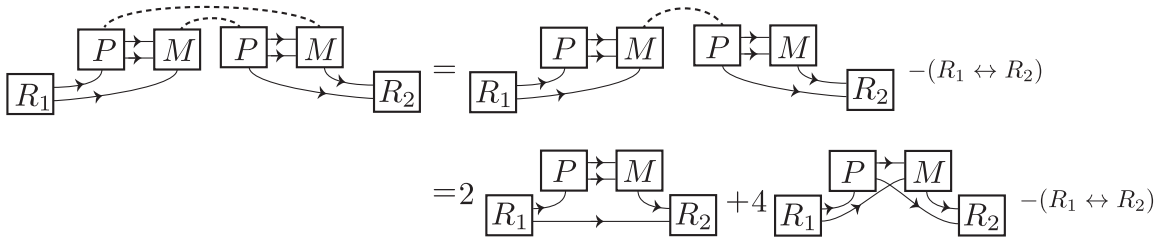


Fig. A1. The graphical computation of $\{J(R_1), J(R_2)\}$.

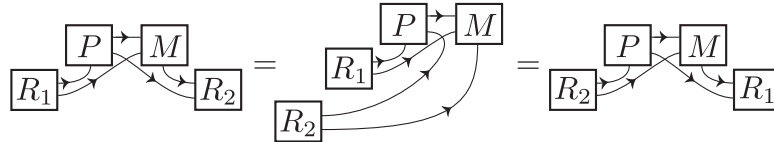


Fig. A2. By using a variant of the identity in Fig. 6, the second graph in the last line of Fig. A1 can be shown to be symmetric under $R_1 \leftrightarrow R_2$.

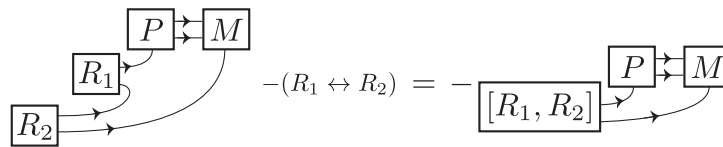


Fig. A3. The final result of the computation of Fig. A1. The first graph can be obtained from the first one in the last line of Fig. A1 by using a variant of the identity in Fig. 6.

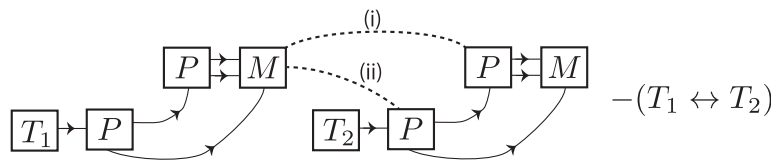


Fig. A4. The computation of $\{H_0, H_0\}$. There are two cases, (i) and (ii), of the fundamental Poisson brackets to be taken.

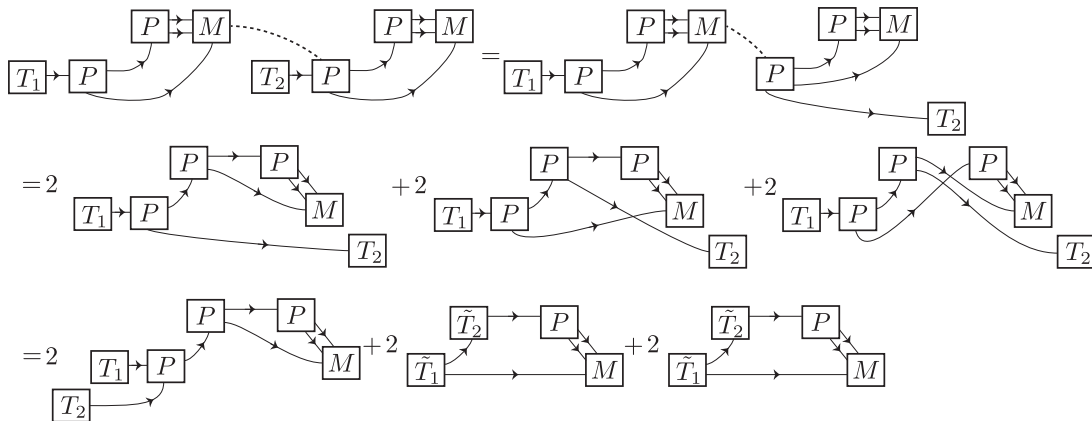


Fig. A5. The computation of the contribution (ii) in Fig. A4.

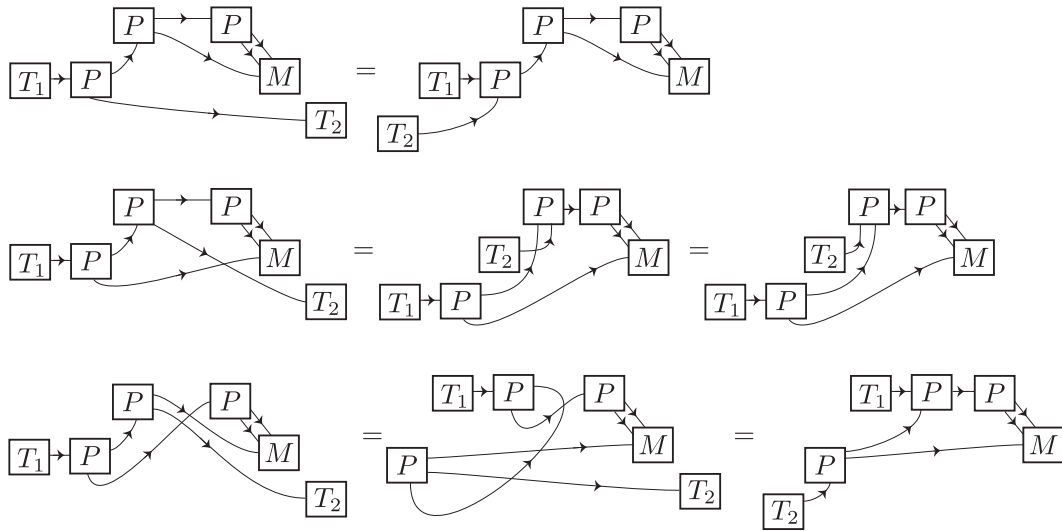


Fig. A6. From the second to the third line of Fig. A5, each diagram is deformed by using variants of Fig. 6 and the symmetry (Fig. 3) of M, P .

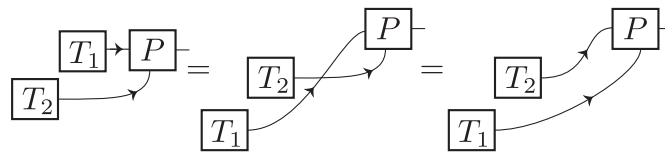


Fig. A7. The first graph of the last line in Fig. A5 is shown to be invariant under $T_1 \leftrightarrow T_2$ by using a variant of Figs. 6 and 3.

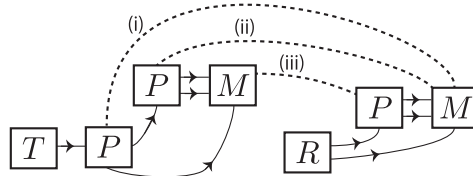


Fig. A8. For $\{H_0(T), J(R)\}$, there exist three cases of the fundamental Poisson bracket being taken.

sum of (ii) and (iii) results in Fig. A3 with the replacement. On the other hand, the computation of the contribution (i) is shown in Fig. A9. By substituting the fundamental Poisson bracket and using some variants of the identity in Fig. 6, we obtain the expression of the last line of Fig. A9. Here the last two terms cancel with the contributions (ii) and (iii), namely, Fig. A3 with $R_1 \rightarrow \tilde{T}, R_2 \rightarrow R$. Therefore, only the first term remains for $\{H_0(T), J(R)\}$. By taking the normalization and the sign of (22) into account, one obtains (24).

A.4. Cosmological constant term

Here we consider the cosmological constant term. The difference between $\{H, H\}$ and $\{H_0, H_0\}$ is

$$\{H(T_1), H(T_2)\} - \{H_0(T_1), H_0(T_2)\} = -\frac{\lambda}{2} \left\{ H_0(T_1), T_2^a M_a^{bc} \Omega_{cb} \right\} - (T_1 \leftrightarrow T_2). \quad (\text{A1})$$

The computation of the first term on the right-hand side can be represented by Fig. A10. There are two contributions (i) and (ii) of the fundamental Poisson bracket. As shown by the graphical computation

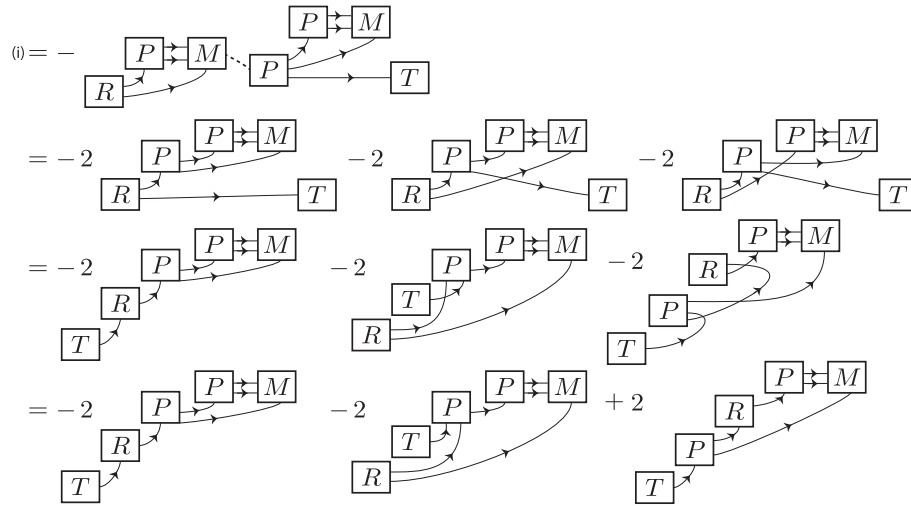


Fig. A9. The computation of the contribution (i) in Fig. A8. In the first line, we perform an exchange of order, $\{J(R), H_0(T)\} = -\{H_0(T), J(R)\}$, and move T to the rightmost position by using a variant of Fig. 6. In the second line, the substitution of the fundamental Poisson bracket (Fig. 8) results in a sum of three terms due to the symmetric property of P . In the third line, some variants of Fig. 6 are used to move T in the first and second terms and T, P in the last term. Finally, by using the symmetric and antisymmetric properties of P and R , respectively, we obtain the last line.

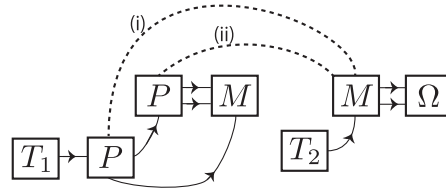


Fig. A10. The computation of $\{H_0(T_1), T_2^a M_a^{bc} \Omega_{cb}\}$. There are two contributions of the fundamental Poisson bracket.

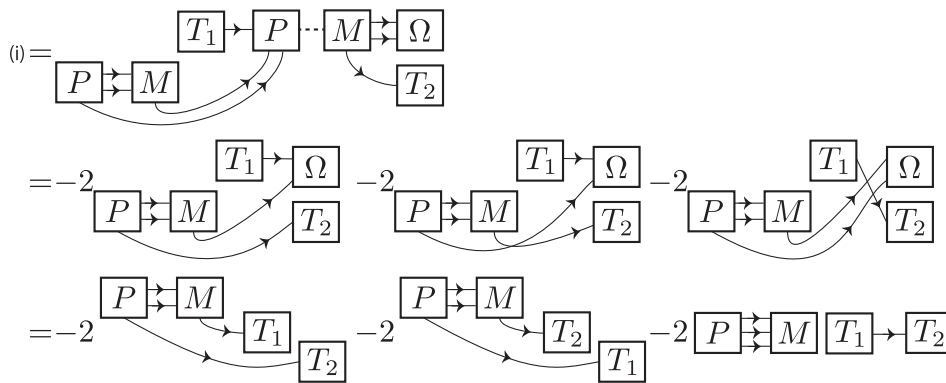


Fig. A11. The computation of (i) in Fig. A10. The result is symmetric under $T_1 \leftrightarrow T_2$, and cancels out.

of Fig. A11, the contribution (i) turns out to be symmetric under $T_1 \leftrightarrow T_2$, and hence cancels out. Here, note that, since Ω is bosonic, we do not need to take the horizontal locations of Ω into account in the graphical expression. The computation of the contribution (ii) is shown in Fig. A12. The second term in the last line is symmetric and cancels out. On the other hand, with the $T_1 \leftrightarrow T_2$ term, the

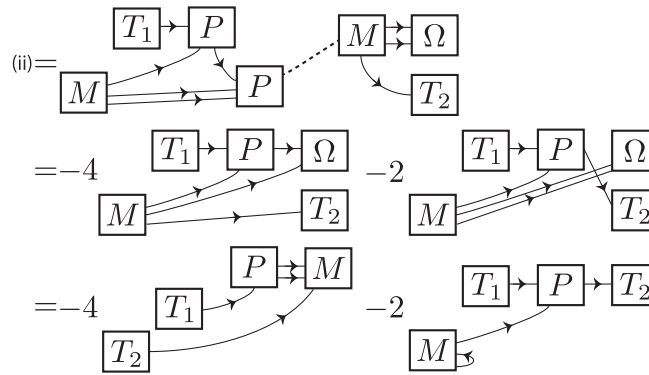


Fig. A12. The computation of (ii) in Fig. A10. The second term in the last line is symmetric under $T_1 \leftrightarrow T_2$, and cancels out. On the other hand, the first term generates the momentum constraint with its $T_1 \leftrightarrow T_2$ term.

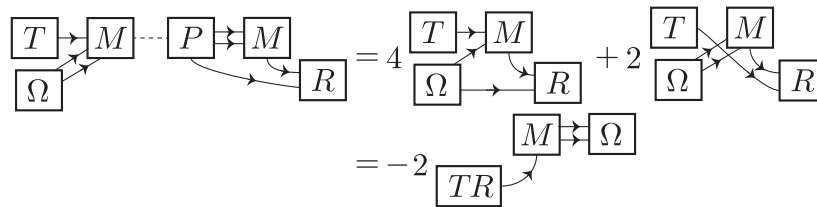


Fig. A13. The Poisson bracket between the cosmological constant term and $J(R)$. The first graph on the right-hand side of the first line vanishes because of the symmetry/antisymmetry properties of M, R .

first term generates $J(2\lambda T_1 \wedge T_2)$ after taking into account the normalization and the sign. This is actually the term proportional to λ on the right-hand side of (23).

We can also check (24). The computation of the additional term proportional to λ is given in Fig. A13.

References

[1] J. Ambjorn, B. Durhuus, and T. Jonsson, *Mod. Phys. Lett. A* **6**, 1133 (1991).
 [2] N. Sasakura, *Mod. Phys. Lett. A* **6**, 2613 (1991).
 [3] N. Godfrey and M. Gross, *Phys. Rev. D* **43**, 1749 (1991).
 [4] M. Fukuma, S. Sugishita, and N. Umeda, [arXiv:1504.03532 [hep-th]] [Search INSPIRE].
 [5] M. Fukuma, S. Sugishita, and N. Umeda, *J. High Energy Phys.* **1507**, 088 (2015) [arXiv:1503.08812 [hep-th]] [Search INSPIRE].
 [6] P. Di Francesco, P. H. Ginsparg, and J. Zinn-Justin, *Phys. Rept.* **254**, 1 (1995) [arXiv:hep-th/9306153] [Search INSPIRE].
 [7] D. V. Boulatov, *Mod. Phys. Lett. A* **7**, 1629 (1992) [arXiv:hep-th/9202074] [Search INSPIRE].
 [8] H. Ooguri, *Mod. Phys. Lett. A* **7**, 2799 (1992) [arXiv:hep-th/9205090] [Search INSPIRE].
 [9] R. De Pietri, L. Freidel, K. Krasnov, and C. Rovelli, *Nucl. Phys. B* **574**, 785 (2000) [arXiv:hep-th/9907154] [Search INSPIRE].
 [10] L. Freidel, *Int. J. Theor. Phys.* **44**, 1769 (2005) [arXiv:hep-th/0505016] [Search INSPIRE].
 [11] D. Oriti, [arXiv:1110.5606 [hep-th]] [Search INSPIRE].
 [12] R. De Pietri and C. Petronio, *J. Math. Phys.* **41**, 6671 (2000) [arXiv:gr-qc/0004045] [Search INSPIRE].
 [13] R. Gurau, *Commun. Math. Phys.* **304**, 69 (2011) [arXiv:0907.2582 [hep-th]] [Search INSPIRE].
 [14] R. Gurau and J. P. Ryan, *Symm. Integ. Geom. Meth. Appl.* **8**, 020 (2012) [arXiv:1109.4812 [hep-th]] [Search INSPIRE].
 [15] D. Benedetti and R. Gurau, [arXiv:1506.08542 [hep-th]] [Search INSPIRE].
 [16] T. Delepouve and R. Gurau, *J. High Energy Phys.* **1506**, 178 (2015) [arXiv:1504.05745 [hep-th]] [Search INSPIRE].

- [17] V. Bonzom, T. Delepouve, and V. Rivasseau, Nucl. Phys. B **895**, 161 (2015) [[arXiv:1502.01365](#) [math-ph]] [[Search INSPIRE](#)].
- [18] T. Delepouve and V. Rivasseau, [[arXiv:1412.5091](#) [math-ph]] [[Search INSPIRE](#)].
- [19] V. A. Nguyen, S. Dartois, and B. Eynard, J. High Energy Phys. **1501**, 013 (2015) [[arXiv:1409.5751](#) [math-ph]] [[Search INSPIRE](#)].
- [20] D. Benedetti and V. Lahoche, [[arXiv:1508.06384](#) [hep-th]] [[Search INSPIRE](#)].
- [21] R. C. Avohou, V. Rivasseau, and A. Tanasa, [[arXiv:1507.03548](#) [math-ph]] [[Search INSPIRE](#)].
- [22] J. B. Geloun, [[arXiv:1507.00590](#) [hep-th]] [[Search INSPIRE](#)].
- [23] V. Lahoche, D. Oriti, and V. Rivasseau, J. High Energy Phys. **1504**, 095 (2015) [[arXiv:1501.02086](#) [hep-th]] [[Search INSPIRE](#)].
- [24] D. Benedetti, J. Ben Geloun, and D. Oriti, J. High Energy Phys. **1503**, 084 (2015) [[arXiv:1411.3180](#) [hep-th]] [[Search INSPIRE](#)].
- [25] J. B. Geloun and R. Toriumi, J. Math. Phys. **56**, 093503 (2015) [[arXiv:1409.0398](#) [hep-th]] [[Search INSPIRE](#)].
- [26] V. Bonzom, R. Gurau, A. Riello, and V. Rivasseau, Nucl. Phys. B **853**, 174 (2011) [[arXiv:1105.3122](#) [hep-th]] [[Search INSPIRE](#)].
- [27] R. Gurau and J. P. Ryan, Ann. Henri Poincaré **15**, 2085 (2014) [[arXiv:1302.4386](#) [math-ph]] [[Search INSPIRE](#)].
- [28] M. Raasakka and A. Tanasa, Ann. Henri Poincaré **16**, 1267 (2015) [[arXiv:1310.3132](#) [hep-th]] [[Search INSPIRE](#)].
- [29] S. Dartois, R. Gurau, and V. Rivasseau, J. High Energy Phys. **1309**, 088 (2013) [[arXiv:1307.5281](#) [hep-th]] [[Search INSPIRE](#)].
- [30] W. Kamiński, D. Oriti, and J. P. Ryan, New J. Phys. **16**, 063048 (2014) [[arXiv:1304.6934](#) [hep-th]] [[Search INSPIRE](#)].
- [31] R. Gurau, Commun. Math. Phys. **330**, 973 (2014) [[arXiv:1304.2666](#) [math-ph]] [[Search INSPIRE](#)].
- [32] J. Ambjorn, J. Jurkiewicz, and R. Loll, Phys. Rev. Lett. **93**, 131301 (2004) [[arXiv:hep-th/0404156](#)] [[Search INSPIRE](#)].
- [33] N. Sasakura, Int. J. Mod. Phys. A **27**, 1250020 (2012) [[arXiv:1111.2790](#) [hep-th]] [[Search INSPIRE](#)].
- [34] N. Sasakura, Int. J. Mod. Phys. A **27**, 1250096 (2012) [[arXiv:1203.0421](#) [hep-th]] [[Search INSPIRE](#)].
- [35] N. Sasakura, Int. J. Mod. Phys. A **28**, 1350030 (2013) [[arXiv:1302.1656](#) [hep-th]] [[Search INSPIRE](#)].
- [36] D. Oriti, [[arXiv:1310.7786](#) [gr-qc]] [[Search INSPIRE](#)].
- [37] R. L. Arnowitt, S. Deser, and C. W. Misner, Phys. Rev. **117**, 1595 (1960).
- [38] R. L. Arnowitt, S. Deser, and C. W. Misner, [[arXiv:gr-qc/0405109](#)] [[Search INSPIRE](#)].
- [39] B. S. DeWitt, Phys. Rev. **160**, 1113 (1967).
- [40] S. A. Hojman, K. Kuchar, and C. Teitelboim, Annals Phys. **96**, 88 (1976).
- [41] C. Teitelboim and J. Zanelli, Classical Quantum Gravity **4**, L125 (1987).
- [42] N. Sasakura and Y. Sato, Phys. Lett. B **732**, 32 (2014) [[arXiv:1401.2062](#) [hep-th]] [[Search INSPIRE](#)].
- [43] N. Sasakura and Y. Sato, J. High Energy Phys. **1510**, 109 (2015). [[arXiv:1506.04872](#) [hep-th]] [[Search INSPIRE](#)].
- [44] N. Sasakura and Y. Sato, Prog. Theor. Exp. Phys. **2015**, 043B09 (2015) [[arXiv:1501.05078](#) [hep-th]] [[Search INSPIRE](#)].
- [45] N. Sasakura and Y. Sato, Prog. Theor. Exp. Phys. **2014**, 053B03 (2014) [[arXiv:1401.7806](#) [hep-th]] [[Search INSPIRE](#)].
- [46] N. Sasakura and Y. Sato, Symm. Integ. Geom. Meth. Appl. **10**, 087 (2014) [[arXiv:1402.0740](#) [hep-th]] [[Search INSPIRE](#)].
- [47] N. Sasakura, Int. J. Mod. Phys. A **28**, 1350111 (2013) [[arXiv:1305.6389](#) [hep-th]] [[Search INSPIRE](#)].
- [48] G. Narain, N. Sasakura, and Y. Sato, J. High Energy Phys. **1501**, 010 (2015) [[arXiv:1410.2683](#) [hep-th]] [[Search INSPIRE](#)].
- [49] N. Sasakura, Prog. Theor. Phys. **119**, 1029 (2008) [[arXiv:0803.1717](#) [gr-qc]] [[Search INSPIRE](#)].
- [50] N. Sasakura, Prog. Theor. Phys. **122**, 309 (2009) [[arXiv:0904.0046](#) [hep-th]] [[Search INSPIRE](#)].
- [51] T. Rempel and L. Freidel, [[arXiv:1507.05826](#) [hep-th]] [[Search INSPIRE](#)].
- [52] B. S. DeWitt, *Supermanifolds (Cambridge Monographs on Mathematical Physics)* (Cambridge University Press, Cambridge, UK, 1992).
- [53] M. Henneaux and C. Teitelboim, *Quantization of Gauge Systems* (Princeton University Press, Princeton, NJ, 1992).